Silicon (2023) 15:609–621
https://doi.org/10.1007/s12633-022-02242-0

ORIGINAL PAPER

# Sensitivity Investigation of Junctionless Gate-all-around Silicon Nanowire Field-Effect Transistor-Based Hydrogen Gas Sensor

**Rishu Chaujar**[1] · **Mekonnen Getnet Yirak**[1,2]

Received: 16 May 2022 / Accepted: 19 November 2022 / Published online: 21 December 2022


**Abstract**
In this work, a junctionless(JL) gate all around (GAA) silicon nanowire field-effect transistor sensor for the detection of hydrogen ($H_2$) has been carried out. The sensors are designed to specify hydrogen gas ($H_2$) existence. Unsafe conditions can result if hydrogen escapes and accumulates in an enclosed space throughout the purifying process; this is why we try to investigate technologically ultra-small-scale hydrogen gas sensor devices. The sensor also showed satisfactory characteristics for ensuring safety when handling hydrogen and remarkable selectivity for monitoring $H_2$, among other gases, such as LPG, $NH_3$, and CO. The temperature and palladium (Pd) gate work function variations in the translation processes are well-thought-out throughout a change in palladium (Pd) gate work function following exposure to the hydrogen gas molecule ($H_2$). Due to its sensitivity to $H_2$ gas, palladium (Pd) is employed as a gate electrode in $H_2$ gas detection. Shift in threshold voltage ($V_{th}$), Ion and Ioff as a result of the metal work function at the gate changing when gas is present; these changes can be regarded as sensitivity parameters for sensing hydrogen gas molecules. ATLAS-3D device simulator has been conducted at low drain bias voltage (0.05V). This study focuses on temperature variation (300K to 500K) and palladium (Pd) metal gate work function variations (5.20eV to 5.40eV) to examine the existence of hydrogen molecule($H_2$) and its effect on the performance of junctionless SiNW-GAA field-effect transistor gas sensors. When the sensitivity $\left(S_{I_{OFF}}\right)$, of proposed JL-GAA-SiNWFETis compared with GAA-MOSFET and bulk MOSFET, JL-GAA-SiNWFET shows improved sensitivity. The results show that as 150mV Pd work function shifts at the gate, the sensitivity improvement with JL-GAA-SiNWFET-based hydrogen gas sensors are 51.65% and 124.51% compared with GAA-MOSFET and MOSFET, respectively. High dielectric oxide ($HfO_2$) and interface oxide ($SiO_2$) is also employed at the gate to overcome electron tunneling. The study of this work proves that a silicon nanowire field-effect transistor with a junctionless gate all around catalytic palladium (Pd) metal gate is the best candidate for sensing hydrogen gas molecules than a bulk metal oxide semiconductor field-effect transistor (MOSFET).

**Keywords** Hydrogen gas-sensor · Junctionless(JL) · Silicon nanowire FET · Gate-all-around (GAA)

## 1 Introduction

Hydrogen is recognized as one of the most significant clean energy carriers and the ultimate fossil fuel candidate and renewable energy source [1] because of its high heat of combustion, low minimum ignition energy, and high combustion velocity. Due to its robust reducing characteristics, hydrogen is also employed in metal smelting, petroleum extraction, semiconductor processing, glass-making, and the daily chemical industry, among other things [2]. It is owing to the growing demand for gas sensing sensors for seismic monitoring applications, environmental monitoring, medical and automotive industries, in addition to domestic usages, such as detecting pollutants, fueling stations, petroleum refineries, and detecting certain types of bacterial infection, which are continuously at high perilous of gas leakage[1–6]. Designing a hydrogen gas sensor based on a GAA-JL-SiNWFET device is an exciting option for gas sensors. It offers low power consumption, high sensitivity, low cost, portability,

✉ Rishu Chaujar
chaujar.rishu@dtu.ac.in

Mekonnen Getnet Yirak
mekonnengetnet01@gmail.com

[1] Applied Physics Department, Delhi Technological University, Delhi, India

[2] Physics Department, Debre Tabor University, Debre Tabor, Ethiopia

technology compatibility, on-chip integration, small size, and CMOS compatibility [7, 8]. Humans cannot smell hydrogen gas since it is colorless and tasteless [9, 10]. It is easily flammable and explosive due to its low explosion energy and extensive flammable range. As a result, an effective and reliable hydrogen sensing device is required for hydrogen manufacturing and consumption, monitoring and managing hydrogen concentrations in nuclear reactors and coal mines, and detecting and alarming $H_2$ leakage during storage, transportation, production and usage [1, 3, 6, 7]. As a result, such sensors seem to be among the most straightforward, inexpensive, and efficient tools for real-time measurement or gas leak detection [10]. Due to various reasons, different types of SiNWFET-based hydrogen gas detecting devices have been designed in recent years to identify gas molecules by analyzing the induced change in work function at the surface of an attractive film [6, 9]. Numerous types of gas detectors are available, but FET-based gas detectors have received much attention [11]. Device engineering is being used in this area of research and development, including modeling and evaluating the field-effect device to improve sensitivity [5]. Floating gate MOSFETs [12], SOI MOSFETs, dual-gate MOSFETs [13], and now nanowire MOSFETs [14] have all been considered in device engineering. A high surface area to volume ratio is necessary to boost sensitivity by raising the potential for surface interactions [8]. Gas sensors in this device depend on the interaction of a thin Pd layer with hydrogen gas [9, 15, 16]. A junctionless nanowire transistor is a gated resistor with the same doping type on the source, channel, and drain without junctions [17]. For example, leakages are always a hazard at gas stations and refineries, and early recognition is thoughtful to minimize dangers and accidents[1, 2]. A silicon nanowire Field Effect Transistor (SiNWFET sensors are an enticing proposition for gas sensing [9] due to technology compatibility) [18] for on-chip integration, portability, low power consumption, and the ability to detect both weakly bound strongly bonded and chemical bonding species at room temperature [19, 20]. The detecting mechanism is the interfacial adsorption of disassociated hydrogen molecules into the palladium gate results in the formation of a dipole layer, which alters the gate's work function and causes a significant shift in threshold voltage ($\Delta V_{th}$) [3, 9, 19]. For example, different catalytic gate metals have been utilized to realize the hydrogen gas sensor, such as Palladium [15, 21], Platinum[1], [7], and poly-methylmethacrylate-platinum[8]. Semiconductors such as silicon nanowires (SiNWs) and thin films have been utilized as sensing materials for the development of high hydrogen gas sensors in recent years [1] [9] due to their huge specific surface area and unique electron transportation characteristics.

Numerous nanoelectronics devices with multiple gate materials, for instance, floating gate MOSFETs [20], Palladium (Pd) gate MOSFETs [22], and Tunnel-FET (TFET) [23], etc., have been designed to boost the sensitivity of SiNWFET based sensors [16]. The planer MOSFET is the most ideal among them because of its production ease, although it has a number of drawbacks in the ultra-small scall dimension, such as short channel effects (SCEs), Subthreshold Swing [24–26]. Under ambient conditions, a junctionless catalytic metal gate-all-around silicon nanowire FET [27–31] device is best for overcoming these issues and providing better performance in terms of sensitivity and response time. Because of a more active surface interaction of hydrogen gas molecules with palladium [19], nanostructure palladium gate materials have a high attraction for hydrogen gas and provide superior sensing capability [22, 32] than bulk palladium materials. Due to these and other physical significance, we employed Nanowire palladium materials as gate electrodes for our proposed device.

In this work, high-k materials for gate oxide, like hafnium oxide($HfO_2$) and interface oxide ($SiO_2$), were chosen to develop new and high-performance electrical devices at the nanoscale that has relied heavily on gate dielectric materials [33–35]. Since hafnium oxide($HfO_2$) provides the most excellent and powerful dielectric materials, enhancing the sensing performance compared to other simulated dielectric materials [33, 36] in controlling tunneling/leakage current. The significance of utilizing Pd metal gate as a catalyst to improve SiNW thin film $H_2$-sensing performance is the straightforward synthesis, which allows for precise control of the thicknesses of SiNW and Pd metal gate to produce detectors with the maximum possible sensitivity [37]. Because palladium electrode selectively absorbs hydrogen gas and produces palladium hydride, as it is employed in various industries [22].

Therefore, we have designed a p-type substrate junctionless gate-all-around SiNWFET-based sensor to investigate hydrogen gas using Atlas-3D-TCAD device simulator tool.

### 1.1 Device structure

The designed structure for our proposed device is illustrated in Fig. 1) here, L (20nm) is the length of dielectric material ($HfO_2$), channel, ($SiO_2$) is an interface oxide layer and $T_1$ $T_2$, and $T_3$ are the thickness of the metal Gate, hafnium oxide, and interface ($SiO_2$) oxides, respectively, and 2R is channel diameter (silicon film thickness), as shown in Table 1. The device gate length is 20nm for all simulations, and source and drain lengths are each 10nm, as shown in Table 1. To achieve a tolerable threshold voltage, a high doping concentration ($1x10^{19}cm^{-3}$) was applied uniformly through the channel

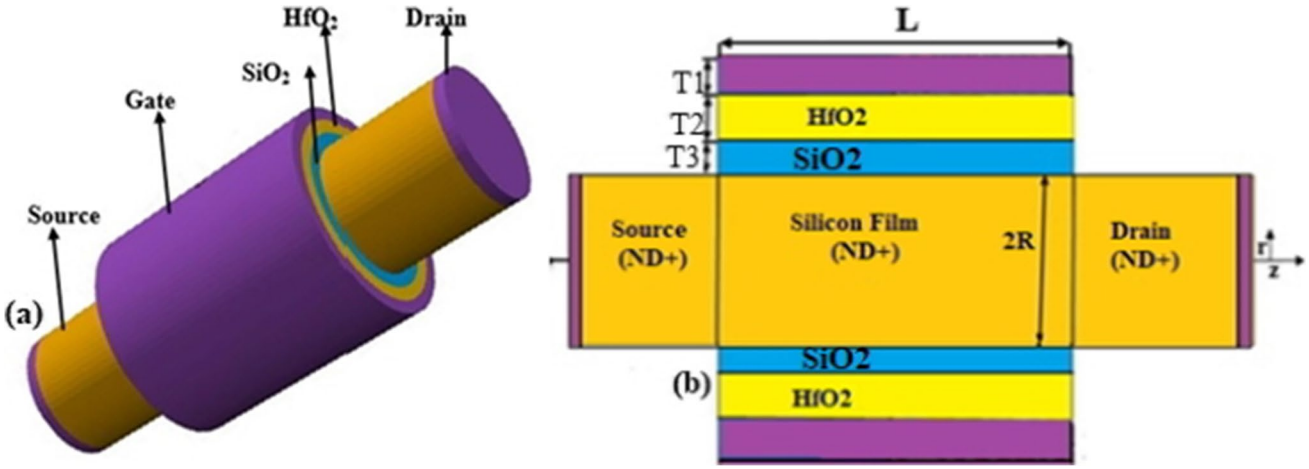


**Fig. 1** illustrates **(a)** 3D representation diagram and **(b)** 2D cross-sectional view for p-type substrate cylindrical JL-GAA-SiNWFET-based hydrogen sensor

**Table 1** Technology parameters

| Device Parameters | GAA-JL-SiNWFET |
|---|---|
| Channel length (nm) | 20.00 |
| Thickness of oxide $HfO_2$ & $SiO_2$ respectively, (nm) | 1.50 & 0.30 |
| Interface Oxide ($SiO_2$) thickness, (nm) | 1.00 |
| Oxide ( $SiO_2$) length, (nm) | 20.00 |
| Source and Drain length/thickness (nm) | 10.00 |
| Hafnium Oxide ($HfO_2$) length, (nm) | 20.00 |
| Radius of silicon film (nm) | 10.00 |
| Drain, Source & Channel Doping ($N_D$+) | $10^{19}cm^{-3}$ |
| Oxide dielectric constant, $HfO_2$ & $SiO_2$ | 25.00 & 3.90 |
| Reference gate work function (Palladium), (eV) | 5.20 |

from the source to drain for our designed p-type substrate devices. The supply gate-source voltage (0.6V) with a consistent drain-source voltage (0.05V) have been employed for all simulations.

## 1.2 Simulation methodology

Silvaco TCAD-ATLAS tool is used for all simulations in this work. Concentration-dependent mobility, drift-diffusion, and field-dependent mobility models are activated to incorporate electron mobility models [38]. To account for the recombination of majority and minority charge carriers, the Shockley-Read-Hall (SRH) recombination model is also activated [39]. The drift-diffusion model also accounts for the driving current caused by the charge carrier following. Due to heavy source and drain doping, Fermi Dirac Statistics have been introduced. The Boltzmann transport statistics and concentration, voltage, and temperature(CVT) [39] Lombardi mobility model [16] have accounted for parallel and perpendicular field mobility [39]. Palladium(Pd) has a high affinity for hydrogen, making it an excellent material for detecting hydrogen storage (reversibly introduced) [10, 40, 41]; when interacting with the palladium surface, Van der Waals forces interact between hydrogen gas molecules and palladium atoms [22].

Figure 1 demonstrates (a) the three-dimensional structures and (b) the two-dimensional cross-sectional view of the p-type palladium metal gate Junctionless (JL) GAA SiNWFET-based hydrogen gas sensor. The GAA SiNWFET structure includes a 40 nm long p-type doped channel and applied $1x10^{19}$ $cm^{-3}$ doping concentration from the source to drain through the channel uniformly. Palladium metals were applied as the gate material because hydrogen molecules at the palladium surface breakdown when $H_2$ gas is exposed to a palladium metal gate, which causes dissociated molecules to diffuse into the gate [10, 22].

In this study, we have considered the catalytic metal gate method to describe the behavior of JL-GAA-SiNWFET based hydrogen gas sensor. The Pd work function must be a critical factor in altering the electrical field properties of the device as it changes [40]. The $H_2$ gas molecules break down at the metal surface of the metal gate (Pd) after exposure to the gas [40], and the disassociated molecules subsequently diffuse within the metal gate, as shown in Fig. 2b**.** Consequently, some hydrogen atoms diffuse through the gate metal, eventually producing the dipole at and within the interface by changing the metal-work function. As a result, we have examined the $\mathbf{I_{ON}/I_{OFF}}$

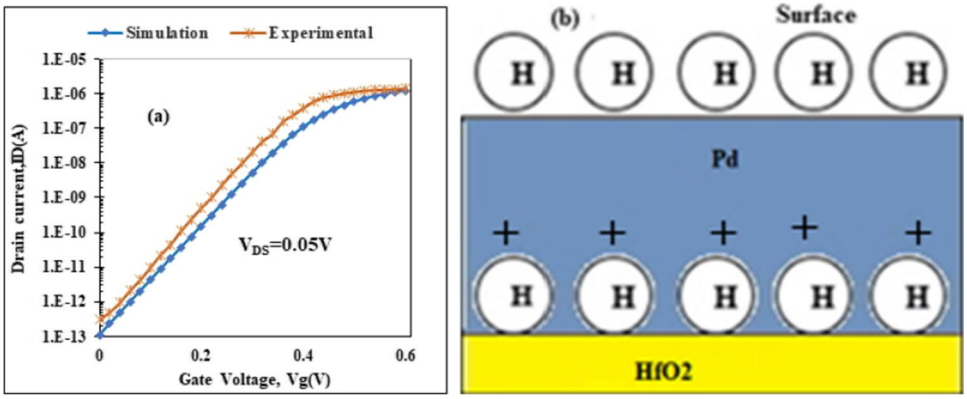


**Fig. 2** illustrates (**a**) Calibration with simulation results at $V_{DS}$=0.05V with the experimental result [42] and (**b**) 2D Electrical dipole generation at the Pd/$HfO_2$ interface

ratio, drain-off sensitivity **($S_{Ioff}$),** and the proposed device's performance shift in threshold voltage.

### 1.3 Analytical modeling

Using boundary conditions, surface potential in the radial direction is obtained;

$$\phi_S(z) = Ae^{kz} + Be^{-kz} + \boldsymbol{\Phi} \tag{1}$$

Here k is described by

$$k = \sqrt{\frac{2\varepsilon_{OX}}{\varepsilon_{Si}R^2\ln\left(1+\frac{t_{OX}}{R}\right)}} \tag{2}$$

And Φ is given by

$$\boldsymbol{\Phi} = V_{gs} - V_{fb} - qN_{Si}/\varepsilon_{Si}k^2 \tag{3}$$

I) As a function of z, the surface potential is given by:

$$\phi(r=0,z) = \phi_c(z) \tag{4}$$

II) At the center of silicon substrate's electric field is zero and expressed as:

$$\left.\frac{\partial\phi(r,z)}{\partial r}\right|_{r=0} = 0 \tag{5}$$

At the boundary of silicon oxide, the electric field is computed as follows:

$$\left.\frac{\partial\phi(r,z)}{\partial r}\right|_{r=\frac{t_{si}}{2}} = \frac{C_{OX}}{\varepsilon_{si}}\left(V_{gs} - V_{fb} - \phi\left(r=\frac{t_{si}}{2},z\right)\right) \tag{6}$$

Oxide capacitance per unit area ($C_{ox}$) is obtained;

$$C_{OX} = \frac{\varepsilon_{OX}}{(R/2)\ln\left(1+\frac{t_{OX}}{R}\right)} \tag{7}$$

Here, $t_{Si}$ is silicon thickness, R is silicon (channel) radius, $\varepsilon_{Si}$is permittivity of silicon, and $\varepsilon_{OX}$ is oxide layer permittivity. The variation in the catalytic metal work function at the metal surface by the reactivity of gas molecules is denoted by $\Delta\Phi_m$, and the flat-band voltage is $V_{fb,}$ and $V_{fb}$ is described by [5, 9];

$$V_{fb} = \phi_m - \phi_{Si} \pm \boldsymbol{\Delta\Phi}_m \tag{8}$$

where $\phi_{Si}$ represents for a silicon work function and is obtained by;

$$\phi_S = \frac{E_g}{2} + \chi + q\phi_{fp} \tag{9}$$

The value of $\Delta\Phi_m$is expressed using Eq. (10)**:**

$$\Delta\phi_M = \boldsymbol{cont.}\left(\boldsymbol{\Phi}_m\right) - \left(\frac{RT}{4F}\right)lnP \tag{10}$$

Where T is for absolute temperature, P is for partial hydrogen gas pressure, R is for hydrogen gas constant, and F is for Faraday's constant. A and B are coefficients obtained using source and drain boundary conditions and determined using the formula;

$$A = \frac{\left(V_{bi}+\phi\right)\left(1-e^{-kL}\right)+V_{ds}}{2\sinh(kL)} \tag{11}$$

$$B = \frac{\left(V_{bi}+\phi\right)\left(e^{kL}-1\right)-V_{ds}}{2\sinh(kL)} \tag{12}$$

As illustrated below, the quasi-fermi-potential changes along the channel direction are used to calculate the drain current from the source to the drain.

$$\phi(r,z) = \phi_S(z) + \frac{C_{OX}}{2\varepsilon_{Si}R}\left(V_{gs} - V_{fb} - \phi_S(z)\right)\left(r^2 - R^2\right) \tag{13}$$

As seen below, the subthreshold current is determined using a 2-D potential relation.

$$I_{sub} = 2\pi R\mu q n_i \frac{\int_{V_S}^{V_d} e^{-qV(z)/KT} dv(z)}{\int_0^L \frac{dz}{\int_0^R e^{q\phi(r,z)/KT} dr}} \quad (14)$$

## 2 Threshold Voltage ($V_{th}$) Modeling

For a p-channel MOSFET device, threshold voltage($V_{th}$) in an enhancement mode can be obtained [43] using Eq. (15).

$$V_{th} = V_{(T,0)} + \gamma\left(\sqrt{|V_{SB} + 2\varphi_F|} - \sqrt{|2\varphi_F|}\right) \quad (15)$$

where $V_{th}$ is the threshold voltage, $2\varphi F$ is the surface potential, $V_{SB}$ is the source-to-body substrate bias, $V_{(T,0)}$ is the zero substrate bias threshold voltage, and ($\gamma$) is a constant body effect parameter given by;

$$\gamma = \left(t_{OX}/\varepsilon_{OX}\right)\sqrt{2q\varepsilon_{Si}N_A} \quad (16)$$

Here, $t_{ox}$ is oxide thickness, $\varepsilon_{ox}$ is the relative permittivity of oxide, $N_A$ is the doping concentration, q is the charge of an electron, and $\varepsilon_{Si}$is the relative permittivity of silicon semiconductors.

Temperature affects the threshold voltage of a CMOS device, in addition to how oxide thickness affects threshold voltage as shown in Eq. (2);

$$\varphi_F = \frac{KT}{q}\ln\left(\frac{N_A}{n_i}\right) \quad (17)$$

Where $n_i$ is the silicon intrinsic doping Parameter, k is Boltzmann's constant, $\varphi_F$ is the contact potential, and T is Temperature[12].

$$n_i = 5.2x10^{15} xT^{3/2} xexp\left(\frac{-E_g}{2KT}\right) \quad (18)$$

Here $E_g$ is the bandgap energy of the silicon channel material. For GAA-JL-SiNWFET, the equation for the threshold voltage depending upon the device's radius is given by Eq. (19) [44].

$$V_{th} = \Delta\varphi + \frac{KT}{q}\ln\left(\frac{8KT\varepsilon_{Si}}{q^2 n_i}\right) - \frac{2KT}{q}\ln\left[R\left(\frac{1+t_{OX}}{R}\right)^{\frac{2\varepsilon_{Si}}{\varepsilon_{OX}}}\right] \quad (19)$$

Here **R** is the device's radius, and the work function difference is $\Delta\varphi$.

Summary of fabrication flowchart for the proposed device[24] Fig. 3.

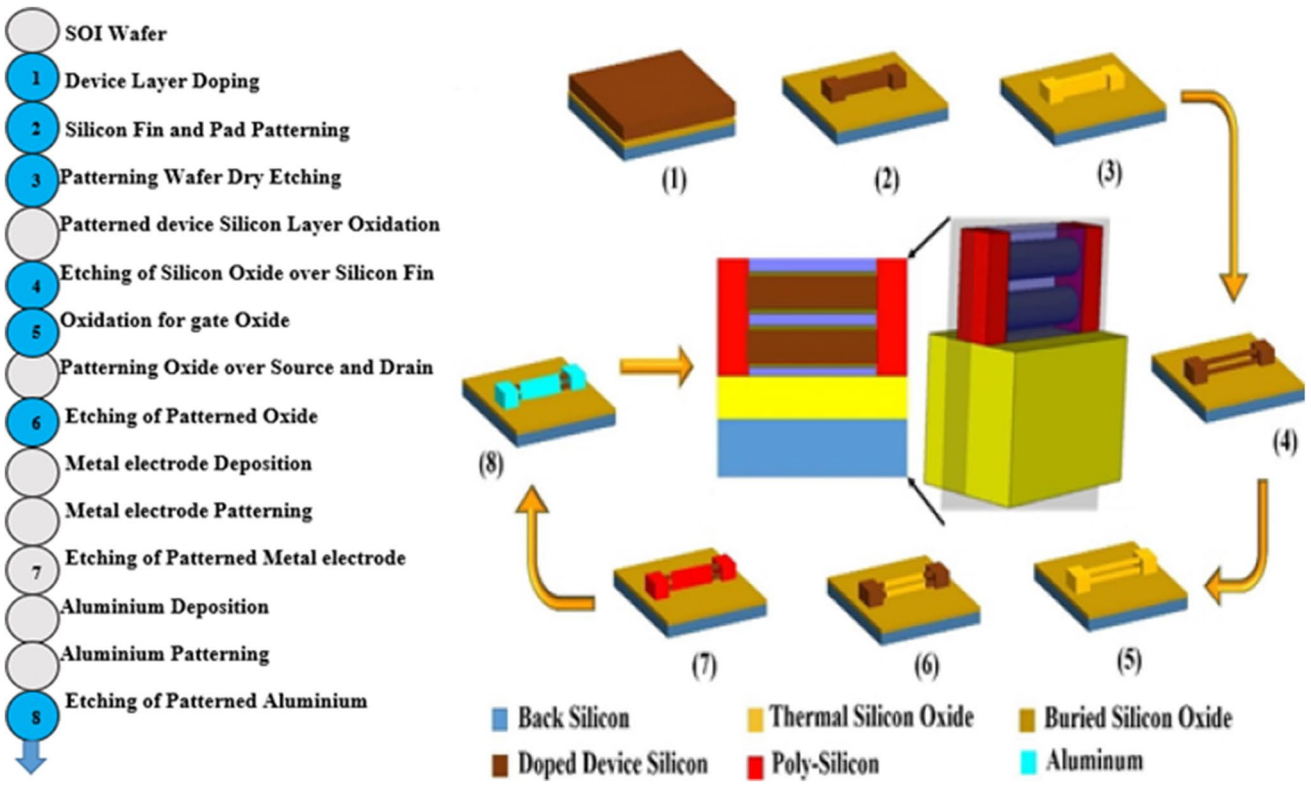


**Fig. 3** Describes the fabrication process flowchart and schematic view for the JL-GAA-SiNWFET fabrication process, adapted [24]

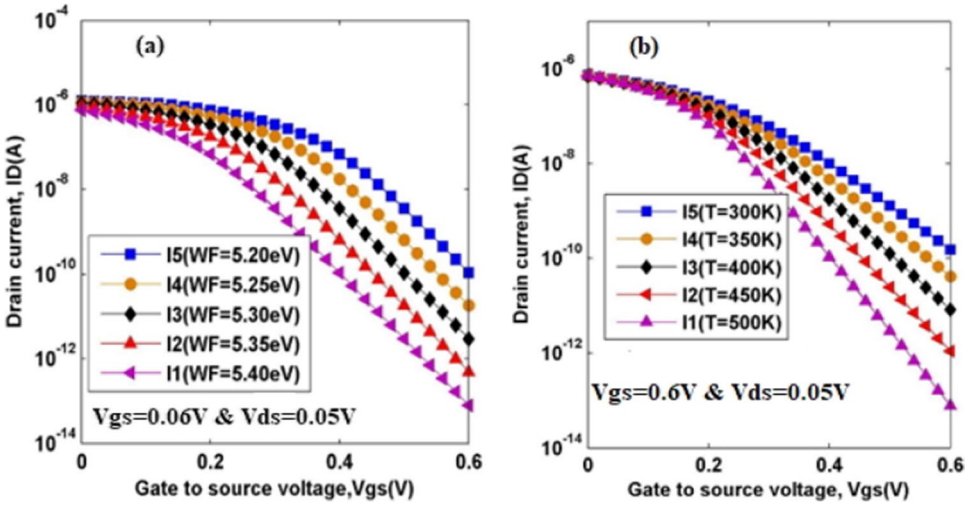


**Fig. 4** illustrates the impact of **(a)** palladium (Pd) work function and **(b)** Temperature on $I_D$-$V_G$ for p-type substrate cylindrical JL-GAA-SiNWFET

## 3 Results and Discussion

### 3.1 Change in drain current

In this work, a change in drain current can also be considered a critical characteristic for identifying hydrogen gas molecules. The change in drain current for a p-type gate-all-around junctionless SiNWFET sensor with a palladium metal gate work function and temperature variation is depicted in Fig. 4. The work function of the catalytic metal gate is controlled by the chemical reaction of hydrogen gas molecules on its surface [22]. In this case, the device's hydrogen gas sensitivity is expressed as a change in the threshold voltage and drain current [20]. For instance, shifting in drain current for the proposed device when the work function changes from 5.20eV to 5.40eV is $1.08x10^{-10}$A and when the temperature varies from 300K to 500K is $1.0x10^{-8}$A, as illustrated in Fig. 4a and b, respectively. In both cases, OFF-current changes rapidly in puny inversion region and is inversely proportional to hydrogen gas concentration due to the impact of metalwork function and temperature variation. As a result, the subthreshold zone provides substantially higher sensitivity while operating at low power, resulting in a low-cost hydrogen gas sensor device. This enhanced sensitivity in the subthreshold region is attributable to different band bending in the nonappearance of Fermi level restraining caused by a shift in palladium metal gate work function following hydrogen gas molecule surface reactivity [9]. We conclude that the proposed device will be desirable for detecting hydrogen gas molecule leaks that could have severe impacts, like an explosion, and the device's sensitivity is obtained Eq. (20).

a) **Change in surface potential**

Figure 5a shows the change in surface potential induced by a shift in the palladium metal work function (5.20 and 5.40 eV). The work function of the catalytic metal gate is altered by the reactivity of hydrogen gas

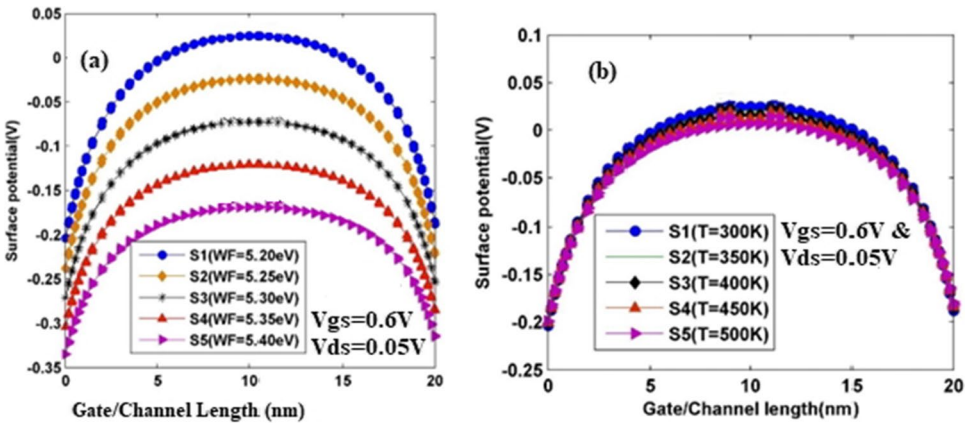


**Fig. 5** impact of **(a)** palladium (Pd) work function and **(b)** Temperature on center potential (V) for p-type substrate cylindrical JL-GAA-SiNWFET

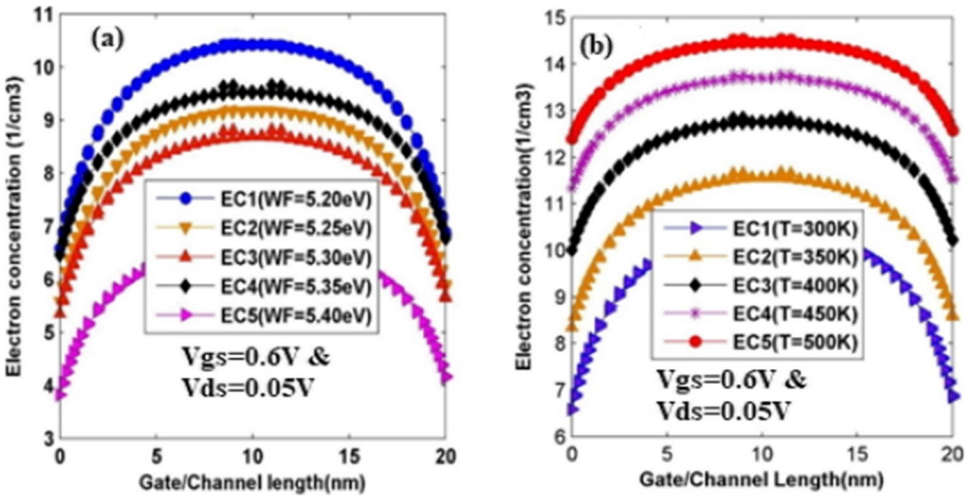


**Fig. 6** influence of **(a)** palladium (Pd) gate work- function and **(b)** Temperature variation on electron concentration (1/cm$^3$) for p-type substrate cylindrical JL-GAA-SiNWFET

molecules at the gate surface, resulting in further band bending and a change in flat-band voltage, as indicated by Eq. (8) [3, 9].

Figure 5a shows that adjusting the work function impacts the surface potential of p-channel junctionless GAA-SiNWFETs with palladium (Pd) metal gates. The work function of the catalytic metal gate is altered by the reactivity of hydrogen gas molecules at the gate surface, resulting in considerable band bending and a shift in flat-band voltage [3, 5], which causes electrical outputs. Such as drain current, surface potential, and threshold voltage ($V_{th}$) shift when the flat-band voltage varies [45]. Using a palladium catalytic metal gate, it is feasible to sense the existence of hydrogen gas molecules by measuring the shifting of $\mathbf{I_{OFF}}$, switching ratio, and $\mathbf{V_{th,}}$ as clearly described in Fig. 6. Variation of temperature also impacts surface potential, as depicted in Fig. 5b) and significantly represents the proposed device sensing capability.

b) **Change in electron mobility**

The electron mobility throughout the channel was also extracted, as shown in Fig. 6. The change in electron concentration due to the shift in palladium metal work function (5.20 and 5.40 eV) is examined in Fig. 6a). The work function of the catalytic metal gate is altered by the reactivity of hydrogen gas molecules at the gate surface, leading to different band bending and a shift in flat-band voltage [3, 9], causing mobility of electrons across the channel. As seen in Fig. 6), the shift in electron concentration in the channel region is substantially more significant than in the source and drain regions. Because the electric field in the channel is affected by electron concentration and the flow of charges in the channel [24]. Figure 6b) shows the impact of temperature on electron concertation for the proposed device.

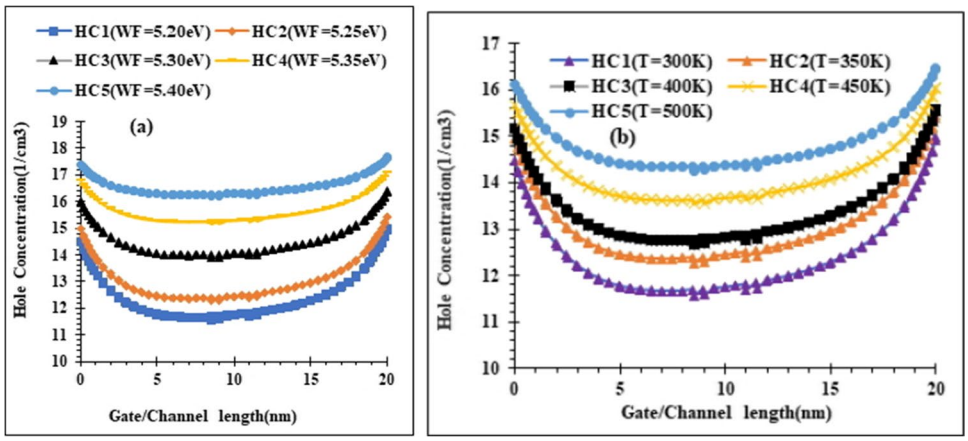


**Fig. 7** effect of **(a)** palladium (Pd) work function and **(b)** Temperature variation on hole concentration (1/cm$^3$) for p-type substrate cylindrical JL-GAA-SiNWFET

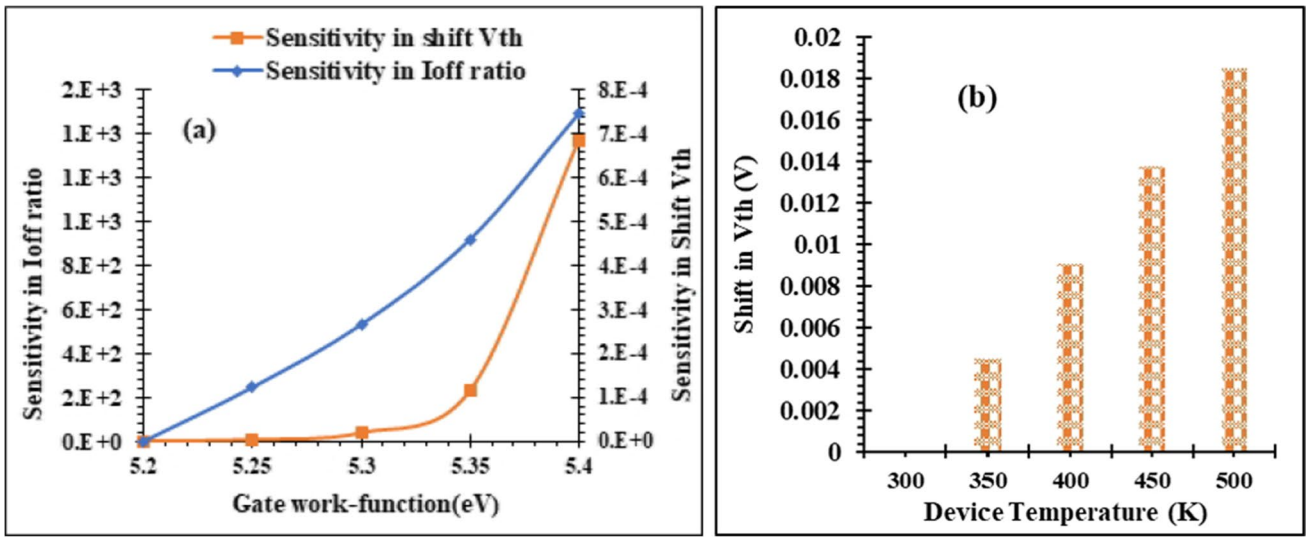


**Fig. 8** effect of **(a)** palladium (Pd) metal gate work and **(b)** Temperature on $I_{OFF}$-current ratio for p-type substrate cylindrical JL-GAA-SiNWFET

### c) Change in hole mobility

The hole mobility throughout the channel was also extracted, as shown in Fig. 7. The change in hole concentration due to the shift in palladium metal work function (5.20 and 5.40 eV) is examined in Fig. 7a). The reactivity of hydrogen gas molecules at the catalytic metal gate surface alters the gate metal's work function, resulting in further band bending and a change in flat-band voltage [3, 9]. As shown in Fig. 7), the channel's hole concentration difference is considerably less than in the source and drain regions. Because the electric field in the channel is affected by hole concentration, the flow of charges in the channel is also influenced, resulting in drain current and, eventually, device sensitivity. The effect of temperature on hole concentration is depicted in Fig. 7b), and device performance should be significant at room temperature. We examine that the proposed technology has shown to be promising for hydrogen gas detection applications.

### d) Shifting in drain current and threshold voltage

The impact of palladium (Pd) work function and temperature variations on device sensitivity are investigated to assess device performance and stability shown in Fig. 8. Figure 8a reflects the sensitivity of gate all around junctionless SiNWFETs as a palladium metal work function in terms of $\mathbf{I_{off}}$ ratio and shift in threshold voltage ($\Delta V_{th}$). It can be shown that gate all around junctionless SiNWFETs has better sensitivity at higher palladium (Pd) metalwork functions [41]. Since the flat-band voltage changes as the palladium gate's metal work function rise due to higher band bending. Due to variations in the palladium metal gate work function, a change in flat-band voltage induces a shift in drain current, threshold voltage(Vth), and [9]. It is thus feasible to identify the existence of hydrogen gas molecules by monitoring changes in $I_{ON}$, $\Delta V_{th}$, and $I_{OFF}$.

Consequently, some hydrogen atoms diffuse through the gate metal, eventually producing the dipole at and within the interface by changing the metalworking function. In this regard, we have examined the $I_{ON}/I_{OFF}$ ratio, drain-off sensitivity **($\mathbf{S_{Ioff}}$),** and shift in threshold voltage of the proposed devices extracting those output results during the simulation, and factors can be regarded as sensitivity variables. We have also shown electron and hole mobility and potential surface distribution along the channel, and carrier transport mechanism has been obtained through NEGF model simulations to obtain the drain current, surface potential, electron and hole mobility and subsequently threshold voltage concerning variation Pd work function and temperature.

When the work function is increased, sensitivity changes exponentially, as seen in Fig. 8a), and it may be estimated using Eq. (20)**.**

$$S_{I_{OFF}} = \frac{I_{OFF(\mathit{after gas reaction})} - I_{OFF(\mathit{before gas reaction})}}{I_{OFF(\mathit{before gas reaction})}} \tag{20}$$

Another essential parameter employed in detecting gas molecules is shifting threshold voltage ($\Delta V_{th}$) and defined as the difference between the threshold voltage with and without hydrogen gas adsorption is defined as ($\Delta V_{th}$) is depicted in Fig. 8) as a function of palladium metal gate work function and temperature. Higher ($\Delta V_{th}$) and $S_{I_{OFF}}$ (shown in Fig. 8) reflects higher palladium metal gate and temperature values, indicating that JL-SiNWFET is well suited for hydrogen gas sensing. As the palladium metal work function

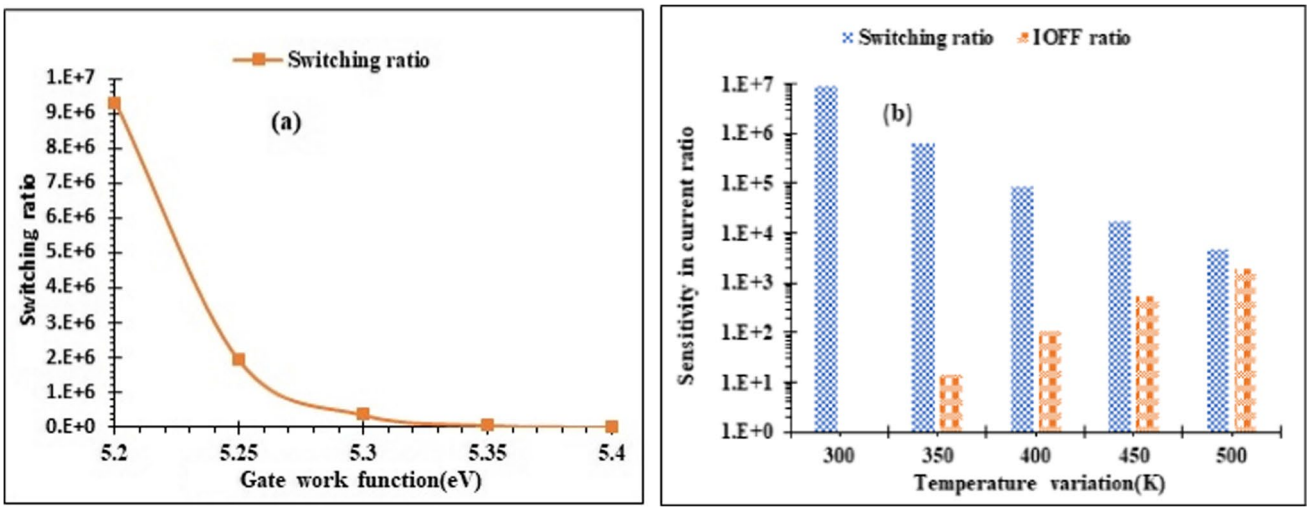


**Fig. 9** effect of **(a)** palladium (Pd) metal gate work function on switching ratio and **(b)** Temperature on shifting threshold voltage for p-type substrate cylindrical JL-GAA-SiNWFET

and temperature increase, a shift in threshold voltage (Vth) arise, resulting in increased hydrogen gas molecule concentration, as seen in Fig. 8), which can be calculated using Eq. (21)**.**

$$\Delta V_{th} = \left| V_{th(\textit{aftergasreaction})} - V_{th(\textit{beforegasreaction})} \right| \tag{21}$$

The impact of palladium (Pd) work function and temperature variations on device switching ratio using different Pd work functions and temperatures to assess device performance and stability as illustrated in Fig. 9. Figure 9a reflects the impact of varying palladium metal work functions on the switching ratio for junctionless gate all around SiNWFETs device. Our proposed device has a lower switching ratio at higher palladium(Pd) metalwork functions. Sensitivity in the switching ratio is lowered as temperature rises (as illustrated in Fig. 9b); sensitivity in terms of $I_{OFF}$ ratio increases as temperature increases (Fig. 9b).

Figure 10 effect of palladium (Pd) work function variation on **(a)** switching ratio and **(b)** leakage current reflects the impact of changing the work function on the switching ratio and leakage current characteristics on our suggested device**.** Figure 10**)** illustrates the analytical model validation with

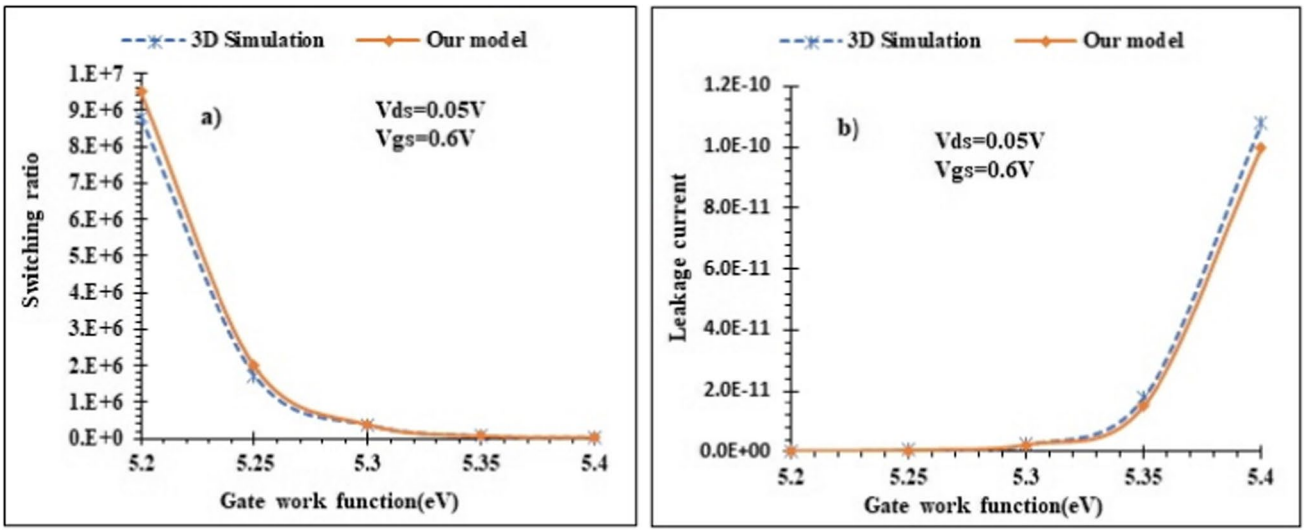


**Fig. 10** effect of palladium (Pd) work function variation on **(a)** switching ratio and **(b)** leakage current for p-type substrate cylindrical JL-GAA-SiNWFET

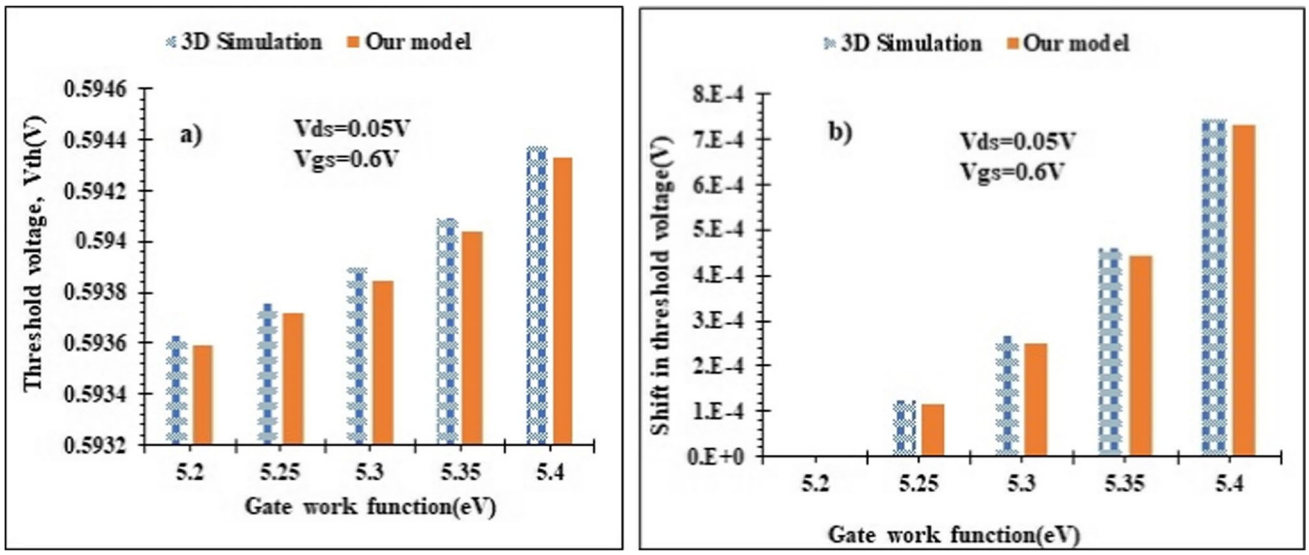


**Fig. 11** impact of palladium (Pd) work function variation on **(a)** threshold voltage ($V_{th}$) and **(b)** shifting on threshold voltage($\Delta V_{th}$) for p-type substrate cylindrical JL-GAA-SiNWFET

the simulation results, which is validated more by the close proximity of our proposed devices.

Figure 11) illustrates the influence of changing the work function on the threshold voltage and shifting threshold voltage characteristics on our suggested device. Figure 11) clearly demonstrates that the analytical model is validated more by the proximity of our proposed device's analytical and simulated results.

Table 2 Examines sensitivity comparison of bulk MOSFET, GAA MOSFET, and JL-GAA-SiNWFET device concerning Off-state current for hydrogen gas sensor after and before gas reaction generated by gas molecules when the threshold voltage of all devices was adjusted at the same

**Table 2** Pd gate sensitivity comparison shows the p-type substrate of bulk MOSFET, GAA-MOSFET, and JL-GAA-SiNWFET

$$S_{I_{OFF}} = \frac{I_{OFF(after\,gas\,reaction)} - I_{OFF(before\,gas\,reaction)}}{I_{OFF(before\,gas\,reaction)}}$$

| | *Previously designed device* [5] | | *Proposed device* |
|---|---|---|---|
| Shifting in Pd work function | Bulk-MOSFET $t_{Si}=20nm$ | GAA MOSFET $t_{Si}=20nm$ R=10nm | JL-GAA-SiNWFET $t_{Si}=10nm$ R=5nm |
| $\Delta\Phi_m=50$mV | 5.08 | 5.96 | 6.17 |
| $\Delta\Phi_m=100$mV | 4.56 | 33.10 | 37.80 |
| $\Delta\Phi_m=150$mV | 102 | 151 | 229 |

Device parameters: Drain, Source, and Channel doping ($N_{Si}$)=$10^{19}cm^{-3}$. Oxide thickness is 1.5&0.3nm, oxide dielectric constants ($HfO_2$ & $SiO_2$ are 25.0 & 3.90, respectively), channel length(L)=40nm, drain to source voltage ($V_{DS}$)=0.05V, gate to source voltage ($V_{GS}$)=0.6V, and radius(R)=5nm.

values. When the sensitivity of JL-GAA-SiNWFET was compared to the sensitivity of bulk MOSFET and GAA MOSFET, the sensitivity was found to be more in JL-GAA-SiNWFET because the sensitivity ($S_{I_{off}}$) equation tells us that the hole mobility is related to the subthreshold leakage current. This provides that the subthreshold current in bulk MOSFET and GAA MOSFET devices is higher than JL-GAA-SiNWFET. Since the JL-GAA-SiNWFET structure experience, a higher surface-to-volume ratio and its channel exposed to more effective gate control than others at gate-source voltage are zero, resulting in a more significant variation in subthreshold current when the work function of the gate metal was altered as the gas molecules react with the catalytic metal gate. For instance, the sensitivity $\left(S_{I_{OFF}}\right)$, of proposed JL-GAA-SiNWFET compared with GAA-MOSFET and bulk MOSFET, JL-GAA-SiNWFET shows improved sensitivity. The results show that as 150mV work function shift of Pd at the gate, the sensitivity improvement with JL-GAA-SiNWFET based hydrogen gas sensors is 51.65% and 124.51% compared with GAA-MOSFET and MOSFET, respectively. Due to high dielectric oxide($HfO_2$) and interface oxide($SiO_2$) suppressing electron tunneling and hole mobility at gate-source voltage vanishes.

Finally, we have summarized the results here; as we have studied different articles, hydrogen is one of the essential future clean energy sources on the road to a more sustainable world and replacing fossil fuels [45, 46]. For instance, the availability of hydrogen may serve as one of the primary drivers of the energy shift and decarbonization [37]. In order to handle hydrogen safely, robust sensors are highly desired. Particularly, it has been shown that the active materials

(Palladium) employed in these sensors exhibit the high sensitivity to $H_2$ required for practical applications and that nanostructuring of these materials enables a reduction in response time of the sensors and a close approximation to the industry standard [22]. Due to these and other applications, we studied and designed a Palladium gate modulated JL-GAA-SiNWFET based hydrogen sensor, and it is crucial in applications where health is of particular significance due to their unique qualities, particularly their innately low fire risk, making them the technology of choice; for instance, in mass transit hydrogen-powered vehicles and $H_2$ accidental leakage [5]. Integrating the palladium electrode in the proposed device enhances device sensitivity performance, lifetime, and reliability. Therefore palladium electrode material is a very sensitive and selective material for $H_2$ and does not require oxygen to carry out [45]**.** For various applications, Palladium JL-GAA-SiNWFET based hydrogen sensor has been examined; since hydrogen is odorless compared to gasoline fuel, it is used for the detection of $H_2$ leakage in the area of hydrogen fueling stations [37], hydrogen pipelines distribution and transmissions [15], cryogenic hydrogen storage tanks(since such storage tanks constantly release $H_2$, leads to change in partial pressure), hydrogen fuel cells (utilized in automobiles and can serve as a backup for generators and small power plants) [41], its water resistance (since, the majority of fuel cells operate with surplus liquids, including water) [20], hydrogen safety and control(increased use of hydrogen fuel leads to more $H_2$ infrastructure incidents) [15], and widely used in industrial settings due to their dependability and excellent sensitivity of $H_2$. Because of the increasing need for hydrogen fuel, efficient hydrogen detection is crucial in many industries for everyday safety and process development. Not only these, Junctionless Gate-All-Around SiNWFET-based hydrogen gas sensor is excellent electrostatic control of short channel effects (SCEs). Due to these and other physical significance, we have studied Palladium integrated junctionless gate all around SiNWFET-based hydrogen gas sensor.

## 4 Conclusion

Through Silvaco-TCAD simulations and analytical model development, this work verified a Junctionless GAA silicon Nanowire transistor with a palladium (Pd) metal gate as a viable sensor for detecting hydrogen gas based on an electrical detecting approach. The resulting analytical model's shifting threshold voltage ($\Delta V_{th}$) and shifting subthreshold current ($S_{IOFF}$) sensitivities are consistent with simulation data. These results indicate higher sensitivity values at higher palladium metal work function and temperature variations due to increased gas surface covering over the Pd metal gate $|\Delta\phi_m|$. We have examined that the catalytic palladium metal gate JL-GAA-SiNWFET sensor has a higher hydrogen gas molecule sensitivity than GAA-MOSFET and conventional bulk MOSFET due to its larger surface-to-volume ratio in addition to improved performance. As is confirmed in Table 2, the percentage improvement in the subthreshold drain current ratio's sensitivity ($S_{I_{OFF}}$) are 124.51% and 51.65% when JL-GAA-SiNWFET compared with bulk MOSFET and GAA-MOSFET, respectively. So, the sensitivity parameter for hydrogen gas sensing in this investigation involves a change in subthreshold current, and it is a critical concern in addition to shifting threshold voltage(($\Delta V_{th}$). This finding provides novel promises for using Pd island gate junctionless gates all around SiNW field-effect transistor sensors to detect hydrogen gas and is applicable for industries such as petrochemical plants, nuclear reactors, hydrogen manufacturing facilities, petroleum refineries, space launching, leak detection, fuel cells, medical diagnostics, and nuclear power plants.

**Supplementary Information** The online version contains supplementary material available at https://doi.org/10.1007/s12633-022-02242-0.

**Acknowledgment** The authors thank Ethiopia's Ministry of Higher Education and Microelectronics Research Laboratory, Delhi Technological University, for supporting the work.

**Data Availability** The authors mentioned above have all relevant data related to this study effort and will be willing to disclose it if asked to do so in the future.

**Authors' Contribution**

All of the authors contributed to the study's inception and design.

**Compliance with Ethical Standards** The authors have reviewed all of the Ethical Standards and are expected to adhere to them in the future.

**Conflict of Interests** The authors declare they have no competing interests.

**Consent to Participate & for the Publication** Since the study report in question is for a 'non-life science journal,' So 'Not Applicable' in this case.

## References

1. Gu H, Wang Z, Hu Y (2012) Hydrogen gas sensors based on semiconductor oxide nanostructures. Sensors (Switzerland) 12:5517. https://doi.org/10.3390/s120505517
2. Kim BJ, Kim JS (2013) Dual MOSFET hydrogen sensors with thermal island structure. Key Eng Mater 543:93. https://doi.org/10.4028/www.scientific.net/KEM.543.93
3. Pratap Y, Kumar M, Gupta M, Haldar S, Gupta RS, Deswal SS (2016) Sensitivity investigation of gate-all-around Junctionless transistor for hydrogen gas detection, 2016 IEEE Int. Nanoelectron Conf 1:1. https://doi.org/10.1109/inec.2016.7589308
4. Cao A, Sudhölter EJR, de Smet LCPM (2013) Silicon nanowire-based devices for gas-phase sensing. Sensors (Switzerland) 14:245. https://doi.org/10.3390/s140100245
5. Gautam R, Saxena M, Gupta RS, Gupta M (2013) Gate-all-around nanowire MOSFET with catalytic metal gate for gas sensing applications. IEEE Trans Nanotechnol 12:939. https://doi.org/10.1109/TNANO.2013.2276394
6. Madan J, Pandey R, Chaujar R (2020) Conducting polymer based gas sensor using PNIN- gate all around - tunnel FET. Silicon. https://doi.org/10.1007/s12633-020-00394-5

7. Kim JS, Kim BJ (2013) Highly sensitive and stable Mosfet-type hydrogen sensor with dual Pt-Fets. Nanosci Nanotechnol Lett 8:43–47. https://doi.org/10.1166/nnl.2016.2097
8. Wang Z, Lee S, Koo K, Kim K (2016) Nanowire-based sensors for biological and medical applications. IEEE Trans Nanobioscience 15:186. https://doi.org/10.1109/TNB.2016.2528258
9. Mokkapati S, Jaiswal N, Gupta M, Kranti A (2019) Gate-all-around nanowire Junctionless transistor-based hydrogen gas sensor. IEEE Sensors J 19:4758. https://doi.org/10.1109/JSEN.2019.2903216
10. Van Toan N, Viet Chien N, Van Duy N, Si Hong H, Nguyen H, Duc Hoa N, Van Hieu N (2016) Fabrication of highly sensitive and selective H2 gas sensor based on SnO2 thin film sensitized with microsized Pd Islands. J Hazard Mater 301:433. https://doi.org/10.1016/j.jhazmat.2015.09.013
11. Sharma B, Kim JS (2018) MEMS based highly sensitive dual FET gas sensor using graphene decorated Pd-ag alloy nanoparticles for H2 detection. Sci Rep 8:1. https://doi.org/10.1038/s41598-018-24324-z
12. Park KY, Kim MS, Choi SY (2015) Fabrication and characteristics of MOSFET protein Chip for detection of ribosomal protein. Biosens Bioelectron 20:2111. https://doi.org/10.1016/j.bios.2004.08.037
13. Sze (2014) Performance investigation of dual material gate stack Schottky-barrier source/drain GAA MOSFET for analog applications. Phys Semicond Devices, Environ Sci Eng 10:739. https://doi.org/10.1007/978-3-319-03002-9
14. Generalov VM, Naumova OV, Fomin BI (2019) Detection of Ebola virus VP40 protein using a nanowire SOI biosensor. Optoelectron Instrum Data Process 55:618. https://doi.org/10.3103/S875669901906013X
15. Najjar YS (2019) Hydrogen leakage sensing and control: (review). Biomed J Sci Tech Res 21(16228). https://doi.org/10.26717/bjstr.2019.21.003670
16. Gupta N, Chaujar R (2016) Influence of gate metal engineering on small-signal and noise behaviour of silicon nanowire MOSFET for low-noise amplifiers. Appl Phys A Mater Sci Process 122:1. https://doi.org/10.1007/s00339-016-0239-9
17. Kumar A, Gupta N, Tripathi MM, Chaujar R (2020) Analysis of structural parameters on sensitivity of black phosphorus Junctionless Recessed Channel MOSFET for biosensing application. Microsyst Technol 26:2227. https://doi.org/10.1007/s00542-019-04545-6
18. Gupta N, Chaujar R (2016) Investigation of temperature variations on analog/RF and linearity Performance of stacked gate GEWE-SiNW MOSFET for improved device reliability. Microelectron Reliab 64:235. https://doi.org/10.1016/j.microrel.2016.07.095
19. Madan J, Chaujar R (2016) Palladium gate all around - hetero dielectric -tunnel FET based highly sensitive hydrogen gas sensor. Superlattice Microst 1. https://doi.org/10.1016/j.spmi.2016.09.050
20. Kim CH, Cho IT, Shin JM, Choi KB, Lee JK, Lee JH (2014) A new gas sensor based on MOSFET having a horizontal floating-gate. IEEE Electron Device Lett 35:265. https://doi.org/10.1109/LED.2013.2294722
21. Sundgren H, Lundström I, Winquist F, Lukkari I, Carlsson R, Wold S (1990) Evaluation of a multiple gas mixture with a simple MOSFET gas sensor Array and pattern recognition. Sensors Actuators B Chem 2:115. https://doi.org/10.1016/0925-4005(90)80020-Z
22. Kumar A (2020) Palladium-based trench gate MOSFET for highly sensitive hydrogen gas sensor. Mater Sci Semicond Process 120:105274. https://doi.org/10.1016/j.mssp.2020.105274
23. Raad BR, Tirkey S, Sharma D, Kondekar P (2017) A new design approach of Dopingless tunnel FET for enhancement of device characteristics. IEEE Trans. Electron Devices 64:1830. https://doi.org/10.1109/TED.2017.2672640
24. Peesa RB, Panda DK (2021) Rapid detection of biomolecules in a junction less tunnel field-effect transistor (JL-TFET) biosensor. Silicon 4. https://doi.org/10.1007/s12633-021-00981-0
25. Veera Boopathy E, Raghul G, Karthick K, Power L, High-Performance MOSFET (2015) International conference on VLSI systems, architecture, technology and applications, VLSI-SATA 2015. Vol. 2(2015). https://doi.org/10.1109/VLSI-SATA.2015.7050455
26. Guerfi Y, Larrieu G (2016) Vertical silicon nanowire field effect transistors with nanoscale gate-all-around. Nanoscale Res Lett 11:1. https://doi.org/10.1186/s11671-016-1396-7
27. Hossain NMM, Quader S, Siddik AB, Chowdhury MIB (2017) TCAD based Performance analysis of Junctionless cylindrical double gate all around FET up to 5nm technology node, 20th Int. Conf Comput Inf Technol ICCIT 2017:1. https://doi.org/10.1109/ICCITECHN.2017.8281858
28. Chowdhury MIB, Islam MJ, Islam MJ, Hasan MM, Farwah SU (2016) Silvaco TCAD based analysis of cylindrical gate -all-around FET having indium arsenide as channel and Aluminium oxide as gate dielectrics. J Nanotechnol Its Appl Eng 1:1
29. Pratap Y, Kumar M, Kabra S, Haldar S, Gupta RS, Gupta M (2018) Analytical modeling of gate-all-around Junctionless transistor based biosensors for detection of neutral biomolecule species. J Comput Electron 17:288. https://doi.org/10.1007/s10825-017-1041-4
30. Getnet M, Chaujar R (2022) Sensitivity analysis of biomolecule Nanocavity immobilization in a dielectric modulated triple - hybrid metal gate - all-around Junctionless NWFET biosensor for detecting various diseases. J Electron Mater. https://doi.org/10.1007/s11664-022-09466-1
31. Chong C, Liu H, Wang S, Chen S, Xie H (2021) Sensitivity analysis of biosensors based on a dielectric-modulated l-shaped gate field-effect transistor. Micromachines 12:1. https://doi.org/10.3390/mi12010019
32. Kumar P, Sharma SK, Balwinder R (2021) Comparative analysis of nanowire tunnel field effect transistor for biosensor applications. Silicon 13:4067. https://doi.org/10.1007/s12633-020-00718-5
33. Kosmani NF, Hamid FA, Razali MA (2020) Effects of High-k dielectric materials on electrical Performance of double gate and gate-all-around MOSFET. Int J Integr Eng **12**(81). https://doi.org/10.30880/ijie.2020.12.02.010
34. Dhiman G (2019) Investigation of junction - less double gate MOSFET with High - k gate - oxide and metal gate layers. Int J Innov Res Sci Eng Technol 8:289
35. Li Q, Zhu H, Yuan H, Kirillov O, Ioannou D, Suehle J, Richter CA (2012) A study of metal gates on HfO 2 using Si nanowire field effect transistors as platform, ECS. Meet Abstr MA2012-02:2614. https://doi.org/10.1149/ma2012-02/31/2614
36. Sarangadharan I, Pulikkathodi AK, Chu C-H, Chen Y-W, Regmi A, Chen P-C, Hsu C-P, Wang Y-L (2018) Review—High field modulated FET biosensors for biomedical applications. ECS J Solid State Sci Technol 7:Q3032. https://doi.org/10.1149/2.0061807jss
37. Koo WT, Cho HJ, Kim DH, Kim YH, Shin H, Penner RM, Kim ID (2020) Chemiresistive hydrogen sensors: fundamentals. Recent Advances, and Challenges, ACS Nano 14:14284. https://doi.org/10.1021/acsnano.0c05307
38. Siddik AB, Hossain NMM, Quader S, Chowdhury MIB (2018) Silicon on metal technology merged with cylindrical gate all around fet for enhanced performance. In: 3rd International Conference on Electrical Information and Communication Technology (EICT). https://doi.org/10.1109/EICT.2017.8275181
39. Ha MW, Seok O, Lee H, Lee HH (2020) Mobility models based on forward current-voltage characteristics of P-Type Pseudo-Vertical diamond schottky barrier diodes. Micromachines 11:598. https://doi.org/10.3390/MI11060598
40. Hung CW, Lin KW, Liu RC, Tsai YY, Lai PH, Fu SI, Chen TP, Chen HI, Liu WC (2007) *On* the hydrogen sensing properties

of a Pd/GaAs transistor-type gas sensor in a nitrogen ambiance, sensors actuators. B Chem 125:22. https://doi.org/10.1016/j.snb.2007.01.027
41. Behzadi pour G, Fekri aval L (2017) Highly sensitive work function hydrogen gas sensor based on PdNPs/SiO2/Si structure at room temperature. Results Phys **7**:1993. https://doi.org/10.1016/j.rinp.2017.06.026
42. Chen ZX, Yu HY, Singh N, Shen NS, Sayanthan RD, Lo GQ, Kwong D (2009) Demonstration of tunneling FETs based on highly scalable vertical silicon nanowires. IEEE Electron Device Lett 30:754
43. Arefin A (2015). Impact of Temperature on Threshold Voltage of Gate-All-Around Junctionless Nanowire Field-Effect Transistor 6:14
44. Sgmosfets SM (2008) Continuous Analytic Current-Voltage ( 1- V ) Model for Long-Channel Doped J ]. 315
45. Choi JH, Jo MG, Han SW, Kim H, Kim SH, Jang S, Kim JS, Cha HY (2017) Hydrogen gas sensor of Pd-functionalised AlGaN/GaN Heterostructure with High sensitivity and low-Power consumption. Electron Lett 53:1200. https://doi.org/10.1049/el.2017.2107
46. Gu H, Wang Z, Hu Y (2012) Hydrogen Gas Sensors Based on Semiconductor Oxide Nanostructures 12. https://doi.org/10.3390/s120505517